ISTITUTO NAZIONALE DI FISICA NUCLEARE

Sezione di Genova

INFN/AE-93/12
25 Maggio 1993

C. Caso:

HEAVY FLAVOR PRODUCTION AND DECAY: AN OVERVIEW

Servizio Documentazione
dei Laboratori Nazionali di Frascati

INFN - Istituto Nazionale di Fisica Nucleare
Sezione di Genova

INFN/AE-93/12
25 Maggio 1993

HEAVY FLAVOR PRODUCTION AND DECAY: AN OVERVIEW[1]

Carlo Caso

Dipartimento di Fisica, Università di Genova and INFN, Via Dodecaneso 33, I-16146 Genova, Italy

Abstract

The experimental status of heavy quark (hadro)production and decay is reviewed, with a special emphasis to the charm meson characteristics. The most recent results are presented; experimental data are compared with theoretical expectations. It is shown that, despite a large experimental activity in the last few years, a lot of work still lies ahead in this domain.

1 INTRODUCTION

Over the last few years the heavy flavor physics has been very active from the experimental (and also from the theoretical) point of view. A large number

[1]Based on two lectures given at the 8th Winter Course of Hadron Physics, Folgaria (TN), Italy, 31 Jan.–6 Feb. 1993

of experiments have been performed with a variety of techniques to investigate the production and decay of charmed and b–flavored particles. My personal opinion is that our present knowledge of the production and weak decay of these particles, although rather "respectable", is not yet fully satisfactory. Since the time allocated to me is limited and the material is very large, I will concentrate on the hadroproduction from fixed target experiments.

This report aims to cover our present (mid 1993) understanding of the experimental situation, together with what theory has elaborated in this field.

2 HEAVY FLAVOR HADROPRODUCTION

2.1 Improved parton model in QCD

The process of heavy quark production in hadronic collisions can be calculated in the perturbative QCD according to the standard factorization formula (see Fig. 1):

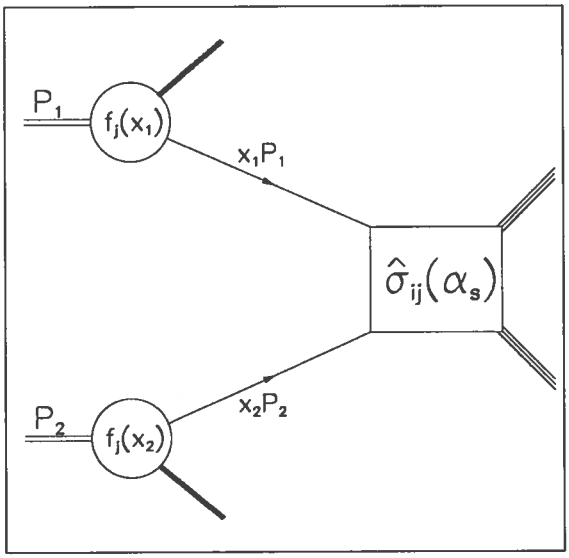

Figure 1: Schematic representation of a hadron–hadron scattering in the QCD parton model.

$$\sigma(P_1, P_2) = \sum_{i,j} \int dx_1 dx_2 f_i(x_1, \mu) f_j(x_2, \mu) \hat{\sigma}_{i,j}(p_1, p_2, \alpha_S(\mu), Q) \qquad (1)$$

where $p_1 = x_1 P_1$ and $p_2 = x_2 P_2$ are the fractional momenta of the colliding partons, $f_i(x, \mu)$ are the structure functions for the i^{th} parton in the incoming hadrons with momenta P_1 and P_2, $\hat{\sigma}_{i,j}$ is the parton short–distance cross section from which the mass singularities are factorized out and μ is the factorization scale for ultraviolet and collinear divergences. The characteristic scale of the hard

scattering is denoted by Q which could be, for example, the mass of the heavy quark produced in the interaction. As the coupling is small at high energies, the short–distance cross section $\hat{\sigma}_{i,j}$ can be calculated as a perturbation series in the running coupling constant α_S. The scale μ is an arbitrary parameter and it should be chosen to be of the order of the characteristic hard scale Q.

The functions $f_i(x,\mu)$ are evaluated at the scale μ and their evolution with energy is given by the equation [1]:

$$\mu^2 \frac{d}{d\mu^2} f_i(x,\mu) = \frac{\alpha_S(\mu)}{2\pi} \sum_k \int_x^1 \frac{dz}{z} P_{ik}(z) f_k(\frac{x}{z},\mu) \tag{2}$$

where again the functions P_{ik} can be written as a perturbation series in the coupling α_S. In formula (1) the two independent scales (the factorization scale μ_F and the renormalization scale μ_R) are fixed to the same value μ.

The running of the coupling constant α_S is determined by the renormalization group equation:

$$\begin{aligned} \frac{d\alpha_S(\mu)}{d\ln\mu^2} &= -b_0\alpha_S^2 - b_1\alpha_S^3 + O(\alpha_S^4) \\ b_0 = \frac{(33-2n_{lf})}{12\pi}, \quad b_1 &= \frac{(153-19n_{lf})}{24\pi^2} \end{aligned} \tag{3}$$

where n_{lf} is the number of light quarks.

The reference scale to apply perturbative QCD is usually expressed in terms of a parameter Λ_{QCD}, which corresponds to energies where α_S is large and defined, in the leading order of α_S, by the relation:

$$\alpha_S(\mu) = \frac{1}{b_0 \ln(\mu^2/\Lambda^2)} \tag{4}$$

One of the most recent evaluations, considering 5 light quarks, turns out to be [2]:

$$150\ MeV < \Lambda^{(5)}_{QCD} < 330\ MeV \tag{5}$$

The leading order [LO, $O(\alpha_S^2)$] processes for the production of a heavy quark Q of mass m (corresponding to quark–antiquark annihilation and gluon–gluon fusion) are:

$$\begin{aligned} &(a)\ q(p_1) + \bar{q}(p_2) \longrightarrow Q(p_3) + \bar{Q}(p_4) \\ &(b)\ g(p_1) + g(p_2) \longrightarrow Q(p_3) + \bar{Q}(p_4) \end{aligned} \tag{6}$$

where the four momenta of the partons are given in brackets. The Feynman diagrams which contribute to the $O(\alpha_S^2)$ are depicted in Fig. 2; the invariant matrix elements squared and the cross–sections for these processes have been known for a long time [3, 4, 5].

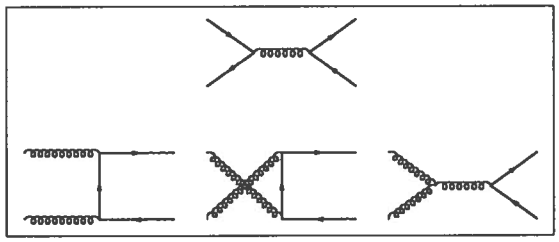

Figure 2: Lowest order Feynman diagrams [$O(\alpha_S^2)$, Born terms] for heavy quark production.

It was early recognized that higher order corrections to heavy quark production could be large: partial $O(\alpha_S^3)$ calculation on quark–gluon fusion has been presented in [6], and single inclusive heavy quark cross–sections at $O(\alpha_S^3)$ are reported in [7, 8]. Recently a full differential computation of the heavy quark cross–section at $O(\alpha_S^3)$ has been given in [9], allowing next–to–leading order (NLO) predictions for any distribution, including correlations. Some of the graphs that contribute to the hadroproduction cross–section at $O(\alpha_S^3)$ level are shown in Fig. 3.

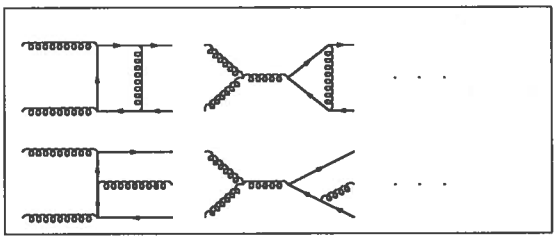

Figure 3: Some of the graphs contributing to the $O(\alpha_S^3)$ level.

In general, the short–distance partonic cross section is parametrized in the form:

$$\hat{\sigma}_{ij}(\hat{s}, m^2, \mu) = \frac{\alpha_S^2(\mu^2)}{m^2} F_{ij}(\rho, \mu^2, m^2) \tag{7}$$

where $\rho = 4m^2/\hat{s}$. This cross–section is then described using the dimensionless functions F_{ij}, whose perturbative expansion is:

$$F_{ij}(\rho, \mu^2, m^2) = F_{ij}^{(0)}(\rho) + g^2(\mu^2)[F_{ij}^{(1)}(\rho) + \bar{F}_{ij}^{(1)}(\rho) \ln \frac{\mu^2}{m^2}] + O(g^4) \tag{8}$$

with $g^2 = 4\pi\alpha_S$. The functions $F^{(0)}, F^{(1)}, \bar{F}^{(1)}$ (corresponding respectively to quark–quark, gluon–gluon and quark–gluon interaction) have been evaluated in

[7] and they show that for high energies, namely in the limit $\rho \to 0$, the dominant processes are gluon–gluon and quark–gluon fusion.

If one wants now to compare theoretical predictions with experimental results he should keep in mind that there are theoretical "errors" associated to the previous formulation, the most important source being due to the truncation of the perturbative expansions. Unfortunately there is no clear way to determine this uncertainty; a possible estimate is obtained varying the scale of the process μ around the mass of the heavy quark; a typical range could be between $m/2$ and $2m$. Since $\mu^2 \frac{d\sigma}{d\mu^2} = O(\alpha_S^{n+1})$ if $\sigma = O(\alpha_S^n)$, this variation gives a lower estimate of the uncalculated higher order terms. In the case of beauty production, one can safely vary both the renormalization and factorization scale independently. For the charm quark there is a further complication connected to its low mass: when computing μ_R around half of the mass of the charm (≈ 0.75 GeV), α_S becomes probably meaningless (although well defined) for such a small scale. Furthermore, as far as μ_F is concerned, there are no structure function parameterizations below the charm mass. Therefore for charm μ_F is usually fixed at twice the charm mass.

As an illustration of this technique, Fig. 4 shows the leading [LO, $O(\alpha_S^2)$] and next–to–leading [NLO, $O(\alpha_S^3)$] results for the total charm and beauty cross sections in π–N interactions as a function of the projectile energy [10]. In Fig. 4 the calculations are performed with $m_c = 1.5$ GeV and $m_b = 4.75$ GeV. The parton distributions for proton and nucleon are taken from [11] while for pion are from [12].

For charm production, the scale uncertainty of both LO and NLO predictions is roughly the same, indicating that there is not a significant improvement when higher terms are considered. On the contrary, for beauty production the width of the uncertainty comes out to be much reduced when NLO terms are added. This expected difference is due to the fact that the higher the mass the smaller α_S is and hence the perturbative expansion becomes more reliable.

There are other sources of uncertainties in the theoretical evaluations of the total cross section, due to the choise of the structure function, the value of Λ_{QCD} and the mass of the heavy quark. The overall allowed ranges for charm and beauty cross sections are reported in Fig. 5 for the variations of the above mentioned parameters as a function of the beam energy [10]. In this figure each band gives the results for a specific value of the quark mass. In particular we notice that the charm cross section is strongly dependent on the charm mass. If the charm mass is moved from 1.2 GeV up to 1.8 GeV, its production cross section is reduced by approximately an order of magnitude. It should be noted that neither intrinsic charm nor flavor excitation are included in the LO calculations, while flavor excitation is considered in the NLO gluon–gluon fusion process. I want also to emphasize that what I do have described so far refers to the production of a heavy quark pair, while experimentally we observe hadrons obtained from these quarks. The "dressing" of quarks into hadrons (hadronization or fragmentation) cannot be calculated in the framework of perturbative QCD, since this process implies

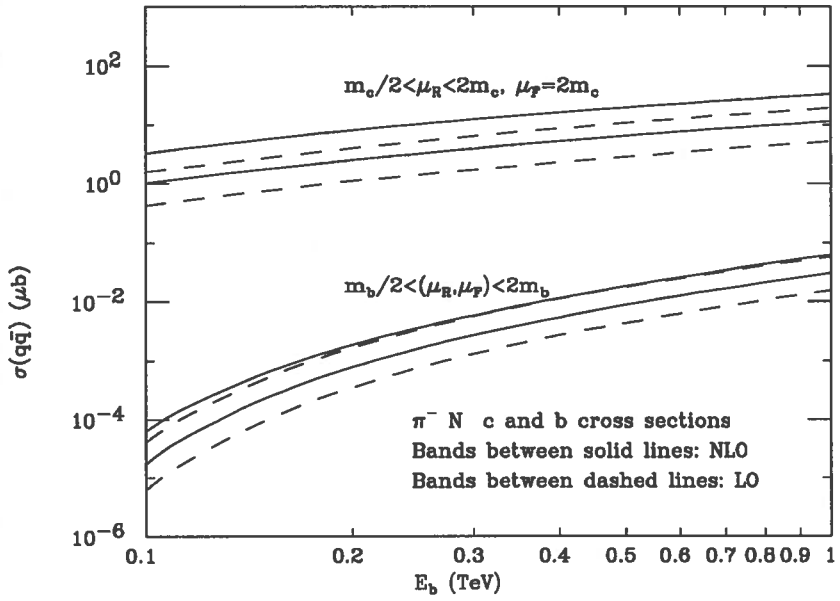

Figure 4: Total cross section at leading and next–to–leading order for charm and beauty production in π–N collisions as a function of the beam energy.

low energies for which α_S is large. The usual way out consists in introducing phenomenological models where the parameters, obtained from the experimental data, are inserted by hand. There are several hadronization schemes on the market (mostly in terms of Montecarlo programs) but their description goes far beyond the limits of these lectures.

2.2 Comparison with experimental data

I am now leaving the enchanting and enchanted castle of theory to enter into immense and hard territory of experimental data. But before making a movement on its ground I want to underline that to perform experiments in heavy quark hadroproduction is like to look for a needle in a haystack. Actually the charm production cross section is only a small fraction of the total cross section. A typical figure of merit is:

$$\frac{\sigma(c\bar{c})}{\sigma_{tot}} \simeq 10^{-3} \tag{9}$$

Furthermore, several other factors are often needed to correct for cuts in the data (trigger and/or particle identification inefficiencies, dead zones in the detectors, limited angular acceptance etc). All these correction factors conspire to reduce

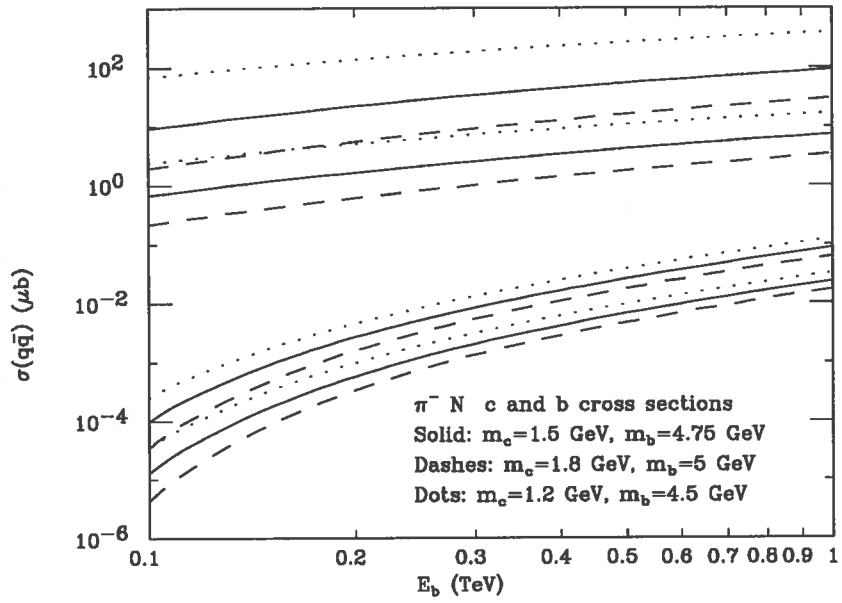

Figure 5: Total cross section for charm and beauty production in π–N collisions as a function of the beam energy. The meaning of the various bands is discussed in the text.

this ratio down to $\sim 10^{-4} \div 10^{-5}$. In spite of that, heavy flavor hadroproduction presents several key points like large production rates, accessibility to all heavy flavors in the final state and a possible use of all kind of beams and targets. The variety of techniques used in the various experiments can be grouped into:

- ♣ indirect measurements (mostly high p_T leptons);
- ♣ emulsions (≈ 2 μm space resolution) coupled to a downstream spectrometer;
- ♣ special bubble chambers (≈ 20 μm space resolution) coupled to a downstream spectrometer;
- ♣ electronic systems, with vertex detectors and triggers.

Table 1 reports the charm hadroproduction results achieved by the most recent experiments. I have marked with a star those experiments having some sort of downstream microvertex detector. From this table one can judge the tremendous improvement obtained with increasing time, mostly connected to both the microvertex technology and computing power.

All these experiments have used a large number of triggers to identify heavy flavor activity in the final state. I would like to summarize these triggers into the following scheme:

Table 1: Main features of the most recent charm hadroproduction experiments.

Experiment	Beam and Target	Year	No. of charms	No. of triggers $\times 10^6$
NA27 (BC) [13]	360 GeV π^-p	1982	183	0.115
NA27 (BC) [13]	400 GeV pp	1984	425	1.0
E743 (BC) [14]	800 GeV pp	1985	134	0.5
WA75 (EM) (*) [15]	350 GeV π^-	1982	288	1.5
E653 (EM) (*) [16]	800 GeV p	1984–85	227	5.4
E653 (EM) (*) [17]	600 GeV π^-	1987–88	676	8.2
NA11 (*) [18]	175 GeV π^- Be	1982	130	6.3
NA32 (*) [19]	200 GeV h^- Si	1984	170	3.8
NA32 (*)[20]	230 GeV π^- Cu	1986	$\approx$ 1,300	17.0
WA82 (*) [21]	340 GeV π^-	1987–9	$\approx$ 3,100	50.0
WA82 (*) [21]	370 GeV p	1988–9	$\approx$ 250	10.0
E769 (*) [22]	250 GeV $h^\pm$	1987–8	$\approx$ 4,000	500.
E791 (*) [23]	500 GeV π^-	1991	$\geq$ 100,000	20,000

- ◊ bubble chambers: only interaction trigger;
- ◊ emulsions: large p_T muons in the final state;
- ◊ particle identification. For instance NA32 has required a pair of unlike–sign particles identified as K or proton. This trigger is especially designed to enrich the sample with $\Lambda_c \to pK^-\pi^+$, $D_s \to K^+K^-\pi$ and more generally with $D\bar{D}$;
- ◊ evidence of secondary vertices. This trigger, used either on–line or off–line, based on the impact parameter criteria that I will describe in a moment, has been widely used as a signature of heavy quark decay;
- ◊ $E_T \geq 5.5$ GeV, where the energy is measured in the calorimeter as for E769 and E791.

The impact parameter trigger takes advantage of the fact that tracks from a secondary decay miss the primary vertex by an amount that depends on the decaying particle lifetime. Defining L e θ as shown in Fig. 6, one has $y = L\sin\theta$. For a relativistic particle, $L = c\tau\gamma$ and since $\sin\theta \sim 1/\gamma$, the average impact parameter results to be $< y >= c\tau$, where τ is the decaying particle lifetime.

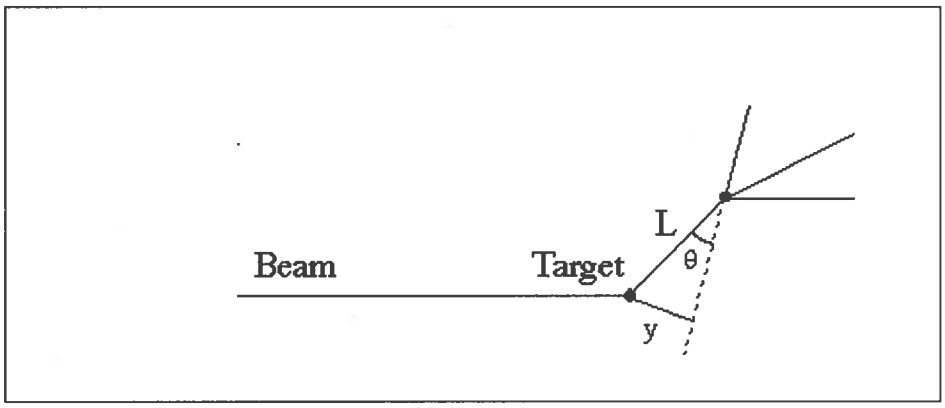

Figure 6: Sketch of the impact parameter definition.

While for charmed hadrons typical values are $< y > \approx 60\ \mu m\ (\Lambda_C^+) \div 320\ \mu m\ (D^+)$, for b–hadrons the average impact parameter is larger than $\approx 350\ \mu$m. Using this on–line trigger with a silicon microstrip telescope made up of 20 μm, 50 μm and 100 μm pitch devices, WA82 has got a D enrichment factor of about 15.

2.3 Total cross sections

Comparison of the total cross section predictions with the experimental data for charm production is reported in Fig. 7 for proton induced reactions (Fig. 7 is taken from [24])[2].

One can see that data and theory agree reasonably well (both in absolute values and in rise with energy) for charm quark masses of the order of 1.5 GeV if higher order corrections are taken into account (LO predictions would indicate a rather low quark mass of $\approx$ 1.2 GeV).

2.4 Longitudinal momentum dependence

Differential cross section shapes do not change appreciably by the addition of the NLO diagrams. By using the so–called Feynman–x variable:

$$x_F = \frac{2p_{||}^{CM}}{E_{CM}} \tag{10}$$

[2]It should be noted that K and π induced reaction cross sections (although still measured in a rather narrow energy range) agree comfortably well with pp data, as expected from theory, since at high energies the gluon–gluon fusion is the most important process.

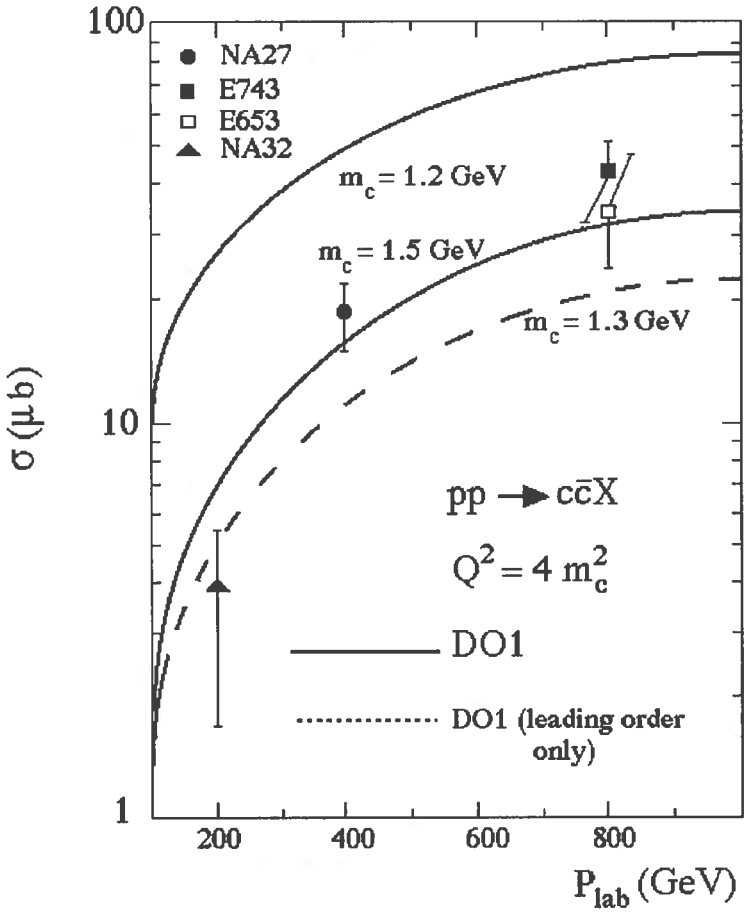

Figure 7: Total charm quark production cross section vs incident proton momentum. The dashed curve is LO calculation with $m_c = 1.3$ GeV. The two solid curves represent NLO calculations with m_c as indicated. The structure functions are from Duke and Owens.

the experimental longitudinal momentum distributions are usually parametrized as:

$$\frac{d\sigma}{dx_F} \propto (1 - |x_F|)^n \qquad (11)$$

There is no theory beyond this formula, but simply a historical reason [25]. From the compilation reported in Table 2 one observes that the meson induced reactions (both π and K) have an exponent n in the range n $\approx 3 \div 5$, while for proton induced reactions n is $\approx 5 \div 8$ (with a possible increase with energy). As a typical example I report in Fig. 8(a) the charm production x_F–dependence as obtained by WA82 [30].

NA27 has pointed out an intriguing problem, the so called "leading particle effect". When separating the D sample into potentially leading states corre-

Table 2: Recent experimental results on x_F and p_T dependence.

Experiment	Beam	Final state	n	b (GeV^{-2})
NA27 [26]	360 GeV π^-	All D	3.8±0.6	1.18±0.17
NA32 [27]	200 GeV π^-	All D	$2.5^{+0.4}_{-0.3}$	$1.06^{+0.12}_{-0.11}$
NA32 [28]	230 GeV π^-	All D	3.74±0.23±0.37	0.83±0.03±0.02
		Λ_c	$3.52^{+0.51}_{-0.49}$	0.84±0.09
		D_S	$3.94^{+0.93}_{-0.86}$	0.59±0.10
E769 [29]	250 GeV π^-	$D^\pm$	3.21±0.24	
		D^0	4.2±0.5	1.09±0.15
WA82 [30, 31]	340 GeV π^-	All D	2.9±0.1±0.3	0.78±0.04
NA32 [27]	200 GeV K^-	All D	4.7±0.9	$2.7^{+0.7}_{-0.5}$
NA32 [28]	230 GeV K^-	All D	$3.56^{+1.08}_{-0.99}$	$1.36^{+0.32}_{-0.26}$
NA27 [32]	400 GeV p	All c	4.9±0.5	1.0±0.1
WA82 [33]	370 GeV p	All D	5.5±0.8	1.27±0.18
NA32 [27]	200 GeV p	All D	$5.5^{+2.1}_{-1.8}$	$1.4^{+0.6}_{-0.4}$
E743 [34]	800 GeV p	All c	8.6±2.0	0.8±0.2
E653 [17]	600 GeV π^-	All D	4.25±0.24±0.23	0.76±0.03±0.03
E653 [16]	800 GeV p	All c	$6.9^{+1.9}_{-1.8}$	$0.84^{+0.10}_{-0.08}$

sponding to D–mesons containing a quark which could be a valence quark of the incoming pion (including the effect of D* production), and non–leading states, with no quark in common with the incoming particle, a very different behaviour is observed. For an incident π^- $(\bar{u}, d)$, D^- $(\bar{c}, d)$ and D^0 $(\bar{u}, c)$ are potentially leading D–mesons, while D^+ $(\bar{d}, c)$ and $\bar{D}^0$ $(\bar{c}, u)$ are non–leading D–mesons. This "leading particle effect" is clearly visible in Fig. 8(b) and Fig. 8(c) which contain the NA27 x_F differential cross sections [26] and it is reflected in a very different value of the exponent n (see Table 3). CCFRS (278 GeV π^- Fe) has also found [35] that the large observed asymmetry between μ^+ and μ^- production can be accounted for with a fraction of the cross section ($\approx 25\%$) consisting of D^- and D^0 produced with fairly flat distribution. More recent data from NA32 [27, 28], E769 [29] and WA82 [31] do not find significant differences between the leading and non–leading states; they all find some indications of the "leading particle effect", although much smaller than the one observed by NA27.

2.5 Transverse momentum dependence

In contrast to other charm hadroproduction properties, the p_T–dependence

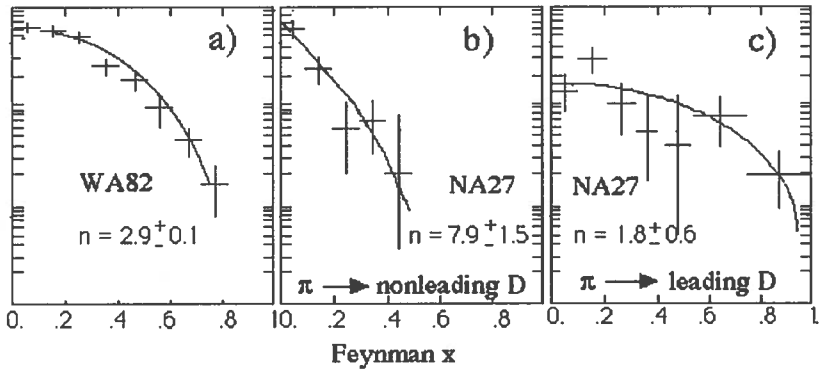

Figure 8: Longitudinal differential cross sections for charm production as obtained by the experiments WA82 (a) and NA27 (b and c). The curves represent fits to the data as explained in the text.

presents much less problems. All the measurements, for almost all charm particles, all targets and all beams, converge towards a unique parameterization of the form:

$$\frac{d\sigma}{dp_T^2} \propto exp\ (-bp_T^2) \tag{12}$$

if the fit is limited to moderate values of p_T^2 ($p_T^2 < 5\ GeV^2$). The experimental data (Table 2) indicate $< p_T > \approx 1$ GeV, in fairly good agreement with a naive QCD prediction of $< p_T > \approx\ m_c$.

2.6 A–dependence

Since many experiments are performed using heavy nuclear targets, the A–dependence (due to nuclear screening effects) is a necessary tool to derive the single nucleon cross section. This permits:

♡ to use solid targets as solid state vertex detectors;

♡ to compare results obtained on different nuclear targets;

♡ to extrapolate experimental results to σ(pp);

♡ to extrapolate results to the theory, which considers only interactions on basic objects.

For light quarks (u, d and s) this A–dependence has been measured using a large variety of final states. Parametrizing the inclusive particle production cross sections in proton induced reactions as:

$$\sigma = \sigma_0 A^\alpha \tag{13}$$

Table 3: Experimental results on the "leading particle effect".

Experiment	Beam	Final state	n
NA27 [26]	360 GeV π^-	Leading D	$1.8^{+0.6}_{-0.5}$
		Non Leading D	$7.9^{+1.6}_{-1.4}$
NA32 [27]	200 GeV π^-	Leading D	$2.1^{+0.5}_{-0.4}$
		Non Leading D	$3.3^{+0.6}_{-0.5}$
NA32 [28]	230 GeV π^-	Leading D	$3.23^{+0.30}_{-0.28}$
		Non Leading D	$4.34^{+0.36}_{-0.35}$
E769 [29]	250 GeV π^-	Leading D	2.84±0.31
		Non Leading D	3.50±0.36
WA82 [30, 31]	340 GeV π^-	Leading D	2.8±0.2±0.3
		Non Leading D	3.7±0.2±0.3

with:

$$\alpha = \alpha(x_F, p_T) \; and \; \sigma_0 \approx 1.5 \div 2.0 \; \sigma(pp)$$

the data show [36] that α depends strongly on x_F, decreasing from ≈ 0.75 at $x_F = 0$ to ≈ 0.45 at $x_F = 1$, and, to a lesser extent, on p_T [37].

For hidden charm hadroproduction an almost linear A–dependence has been proven to be experimentally true ($\alpha = 0.920 \pm 0.008$) from a very high statistics J/ψ and ψ' production experiment [38]. A neutrino beam dump experiment at Fermilab [39] has measured the A–dependence comparing the rates of prompt ν_e and $\bar{\nu}_e$ (arising from charm decay) in Be, Cu and W and has determined $\alpha = 0.75 \pm 0.05$. Corroborating evidence comes from a CERN beam dump experiment (WA78 [40]), where the A–dependence was studied comparing the yield of prompt single muons from a 320 GeV π^- beam on three different target materials Al, Fe and U. The WA78 result is $\alpha = 0.80 \pm 0.05$. It should be pointed out, however, that these indirect measurements are model dependent and need large correction factors.

This result would be fine, since among other things it would help in reducing the large increase in charm production cross sections between the accelerator and ISR energies. However, when trying to compare cross sections at similar energies with those obtained by the small hydrogen bubble chamber LEBC (these are the only available data on hydrogen) one encounters the unexpected problem [41, 42, 16] that a value of $\alpha \approx 1$ is necessary. One has also to keep in mind that a naive QCD prediction would indicate $\alpha = 1$ (since $\sigma \approx N_{partons}$ and hence $\sigma \approx N_{nucleons}$).

Recently we have got two direct measurements of this A–dependence. Both experiments have used different targets in the same set–up and at the same time, thus eliminating most of the systematic uncertainties due to the different experimental conditions of the various targets in the beam dump experiments:

⇒ WA82 [43]: the beam impinges on a thin target divided vertically in two equal sections made up of different materials and the beam is steered such that both sections receive approximately the same intensity. The exact beam profile is determined from the off–line analysis. With a 340 GeV π^- beam into W/Si and W/Cu targets, WA82 finds:

$$\alpha(D) = 0.92 \pm 0.06 \quad 0 < x_F < 0.7 \quad < x_F > = \ 0.24$$

⇒ E769 [44] uses a slightly different method, since the target is made up of 26 thin metal foils located sequentially and crossed by the beam at the same time. This experimental procedure does not require a very precise knowledge of the beam profile (as for WA82); there is however a larger background due to secondary interactions simulating charm decays. With 4 different target materials (Be, Al, Cu and W) and using a 250 GeV π^- beam, E769 finds:

$$\alpha(D) = 1.02 \pm 0.05 \quad 0 < x_F < 0.5$$

This value is a weighted average of consisting results from neutral and charged D separately (D^+: $\alpha = 1.04 \pm 0.08$; D^0: $\alpha = 0.99 \pm 0.10$).

In a word I would say that both results are in quite good agreement. With these new direct and consistent measurements it seems today difficult to believe in large deviations from $\alpha = 1$. Furthermore these recent data confirm the same A–dependence for hidden and open charm and shed also light on the applicability of QCD.

Both experiments have also tried to investigate a possible dependence of α_{charm} on x_F, as suggested by the above mentioned light quark behaviour. Although they do not cover the full x_F range and the statistics is rather poor, there is no indication of any significant dependence.

2.7 Beauty hadroproduction

As already anticipated, I will not spend much time on this item. The b physics potential of hadron colliders is becoming evident. The predicted cross sections are very high [6, 7, 8] and measurements done by UA1 [45] and CDF [46] seem to confirm the QCD predictions. Also the CDF prospects for exclusive channels are appealing and a lot of heavy flavor physics is expected from it in the next few

years with an increase of efficiency and tagging capability (but top priority will certainly be the top hunting). Also the LEP experiments have heavily used the b physics as a unique experimental test of the electroweak model (see for instance [47]).

From fixed target hadroproduction experiments we have had so far a very poor contribution to the b physics. The long–awaited direct observation of a pair of beauty particles decaying into charms has been for years a single clean $b\bar{b}$ event observed by WA75 [48] and fully reconstructed in the emulsion. Unfortunately this example was not followed by any other candidate.

Recently the Hybrid Emulsion Experiment E653 has presented the first results [49, 50] from a sample of 9 $b\bar{b}$ pairs (where b stands for a generic beauty meson or baryon) produced by a 600 GeV π^- beam. This collaboration has adopted a complex stategy to reduce the 10^7 triggers to few 10^4 emulsion scan candidates and the off–line trigger consists in selecting events with $p_T^\mu > 1.5$ GeV/c. Out of 359 events where the high–p_T muon miss the primary vertex, they found 9 $b\bar{b}$ pairs (with an estimated backgroung of ≈ 0.3 events), 175 charm decays (122 found with partner) used for checking purposes, while the rest was attributed to strange decays, obvious or probable interactions etc. The most salient characteristics derived from these 18 b–flavored particles (12 neutral and 6 charged) are the following:

- $\oplus$ $\sigma_{b\bar{b}} = 33 \pm 11 \pm 6$ nb/nucleon (assuming A^1 dependence). The pairs tend strongly to be produced back–to–back;
- $\oplus$ the coefficients n and b obtained from the longitudinal and transverse beauty momentum distributions are respectively $5.0^{+2.7+1.7}_{-2.1-1.7}$ and $0.13^{+0.05+0.02}_{-0.04-0.02}$ $(\mathrm{GeV/c})^{-2}$;
- $\oplus$ the lifetimes (beauty momenta are estimated by Montecarlo) are as follows:
  1. 12 neutral (a mixture of B_d, B_s and Λ_b): $\tau = 0.81^{+0.34+0.09}_{-0.22-0.02}$ ps;
  2. 6 charged (mostly B_u, since only few B_c and Ξ_b are expected): $\tau = 3.84^{+2.73+1.39}_{-1.36-0.15}$ ps;
  3. 18 total: $\tau = 1.86^{+1.13+0.52}_{-0.61-0.02}$ ps.

  One sees immediately that the E653 lifetime results pose a problem: while CLEO [51] and ARGUS [52] find nearly equal semileptonic branching fractions for charged and neutral B's ($\Gamma_l(B^+)/\Gamma_l(B^0) = 0.93 \pm 0.16$ [53]), the above quoted results are very different to each other. Does it imply that B_s and Λ_b [not produced at $\Upsilon(4S)$] are expected to have shorter lifetimes or is it simply a statistical fluctuation? Please note that also the absolute lifetime values are somehow below and above the world averages.

The collaboration is continuing the scanning and they claim for a double sample soon; at that moment all these problems will certainly be addressed better than with the present small statistics.

WA92 (the successor of WA82 at CERN) is currently on the way of processing its 90 million triggers; some tests have already shown the possibility of reconstructing b particles and results are expected soon. Let us wait and see.

3 HEAVY FLAVOR DECAY

3.1 Decay mechanisms of charm particles

In the standard model the charm quark decays via the weak charged current into either the strange or the down quark.

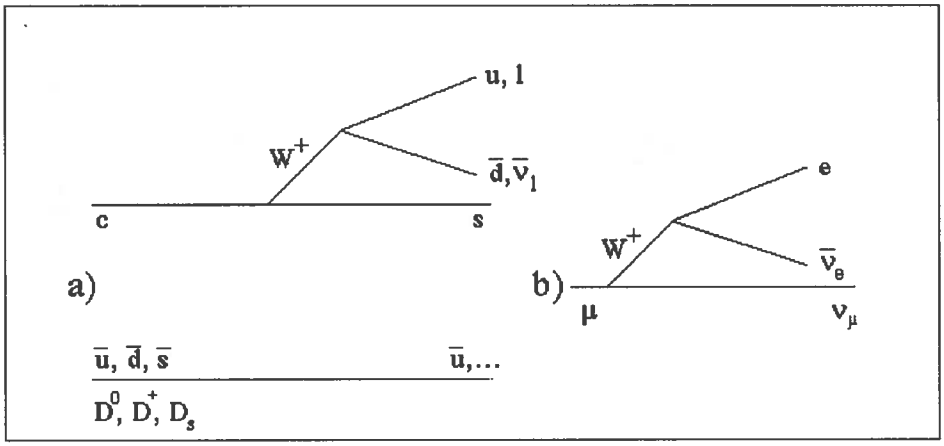

Figure 9: Pictorial representation of: a) spectator diagram for a semileptonic and hadronic decay of a charm meson; b) muon decay diagram.

Fig. 9(a) shows a sketch of a Cabibbo–favoured ($\Delta C = \Delta S = 1$) charm meson decay. Similar diagrams can be drawn both for charm baryons and Cabibbo–suppressed decays (Cabibbo–suppressed decays occur when the virtual gauge boson W goes into a $u\bar{s}$ rather than into a $u\bar{d}$ and/or when the c quark decays into a d quark rather than into an s quark). This diagram is the so–called "spectator diagram" since only the charm quark undergoes a decay, while its partner light quark acts as a spectator; this mechanism is considered to be the dominant decay diagram. Charm quark can also decay via a non standard model mechanism $c \rightarrow X^0 u$ followed by the X^0 decay into a lepton pair or a $q\bar{q}$ pair. MARK II [54] has looked for this $\Delta C = 1$ weak neutral current decay and has found BR($D^+ \rightarrow \pi^+ e^+ e^-$) $< 2.5\ 10^{-3}$ (90% C.L.); therefore this possible non S.M. mechanism will not be considered any longer here.

Since the spectator diagrams are essentially the same for all charmed state decays, one could simply deduce that all charm particles must have the same

lifetime. This lifetime can be estimated comparing the spectator diagram to the muon decay diagram of Fig. 9(b). This comparison predicts :

$$\tau(c) \approx 1/5\ (m_\mu/m_c)^5\ \tau(\mu) \tag{14}$$

and then $\tau(c) \approx 3.5 \div 7.5\ 10^{-13}$ s depending on the mass of the c–quark. Furthermore, since:

$$\tau \sim 1/\Gamma_{tot}\ , B_l = \Gamma_l\ (D \to l\nu X)/\Gamma_{tot}(D \to all) \tag{15}$$

and

$$\Gamma_l\ (D^0 \to l\nu X) = \Gamma_l\ (D^\pm \to l\nu X) \tag{16}$$

one can deduce that all charm particles must also have the same semileptonic branching ratio.

A naive numerical estimate of $B_l \approx 20\%$ is simply given by the three colors and two leptons in which the W of Fig. 9(a) can decay. QCD corrections (gluon exchange between the quark lines) actually reduce the expected branching ratio for semileptonic decay to $\approx 12 \div 15\%$ [55].

The world average values [53]:

$B_l\ (\mathrm{D}^0 \to e^+\mathrm{X}) = (7.7\pm1.2)\%$ $\quad \tau(D^0) = (4.20\pm0.08)10^{-13}$ s

$B_l\ (\mathrm{D}^+ \to e^+\mathrm{X}) = (17.2\pm1.9)\%$ $\quad \tau(D^+) = (10.66\pm0.23)10^{-13}$ s

show that this simple scheme of a pure light quark spectator model is in strong disagreement with the data. However the same data support that the semileptonic widths are consistent with being equal for $D^\pm$ and D^0. The discrepancy is then inside the hadronic decay rates. Before addressing this problem I have to underline that there are other diagrams for a charm particle decay. These diagrams are depicted in Fig. 10:

- ⊗ internal (color–suppressed) spectator diagram. Fig. 10(a) shows such a diagram for D^0, D^+ and D_s decay (I have drawn only the hadronic W decay mode). The contribution of this diagram is expected to be lower by a factor of three in amplitude (and hence a factor of 9 in rate) w.r.t the equivalent normal spectator diagram since the quarks from the virtual W materialization (W does not see the color) must have the same color as the quarks in the initial state in order to pair correctly to produce a final state hadron. The hadronic decay mode $D^0 \to \bar{K}^0\pi^0$ can only go through this internal spectator diagram (although this statement could be criticized on the basis of final state interactions $D^0 \to K^-\pi^+ \to \bar{K}^0\pi^0$); however the measured hadronic modes [53] BR $(D^0 \to \bar{K}^0\pi^0) = (2.1\pm0.5)\%$ and BR $(D^0 \to K^-\pi^+) = (3.65\pm0.21)\%$ provide a ratio 0.58 ± 0.14 much higher than the expected 1/18 (this is a factor two smaller than 1/9 since there is an extra factor $1/\sqrt{2}$ in the π^0 wave function);

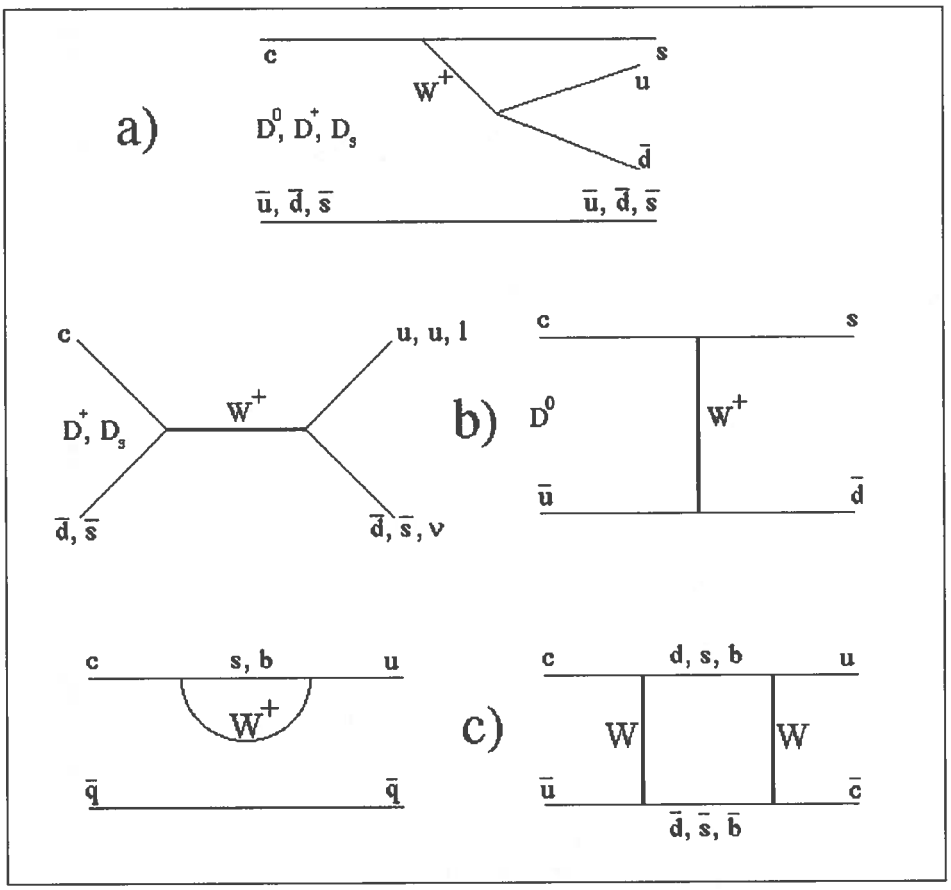

Figure 10: Other decay diagrams for charm mesons: a) internal (color–suppressed) spectator diagram for a hadronic decay; b) annihilation and W–exchange diagrams; c) penguin and mixing diagrams.

⊗ non–spectator diagrams: Fig. 10(b) shows the annihilation diagram for a D^+ (D_s) meson and a W–exchange diagram through which D^0 can decay. In the earlier calculations both these contributions were disregarded due to the helicity conservation which does not allow the coupling of the vector boson W to the pseudoscalar state $c\bar{q}$ (it is the same reason why the π decay mode $\pi^- \to e^-\bar{\nu}$ (although favoured by phase space) is $\approx 10^{-4}$ times smaller than $\pi^- \to \mu^-\bar{\nu}$). However this suppression can be recovered taking into account emission of gluons by one of the initial quarks. The possibility of non–spectator contributions seems to be confirmed by the experimental observation of the decay mode $D^0 \to \phi\bar{K}^0$ which is believed to occur uniquely via the W–exchange diagram. However, as for the color–suppressed diagram, it has been argued [56] that this final state can also be reached via a multichannel final state interaction. Annihilation diagram

contributions are expected to be small and the decay which has a sizeable rate is $D^+ \to \mu^+\nu$. The measurement of this leptonic decay provides the decay constant f_D of the pseudoscalar meson D; if helicity suppression holds, this rate is given by:

$$\Gamma(D^+ \to l\nu) = \frac{G_F^2 \mid V_{c\bar{q}} \mid^2}{8\pi} f_D^2 m_l^2 m_D (1 - \frac{m_l^2}{m_D^2})[1 + \frac{\alpha}{2\pi}(B + B_{SD})] \quad (17)$$

The term of order α contains an inner bremsstrahlung part B, which does not depend on the structure of the meson, and a structure–dependent part B_{SD}. Using the upper limit from MARK III [57] BR $(D^+ \to \mu^+\nu) < 7.2 \times 10^{-4}$ (90% C.L.), one obtains for the D decay constant $f_D < 310$ MeV (90% C.L.);

⊗ finally Fig. 10(c) shows the "penguin" and "mixing" diagrams. While penguin amplitudes are expected to be very small in charm decay, mixing in the $D^0 \Leftrightarrow \bar{D}^0$ system has never been experimentally observed.

3.2 Hadronic decays of charm particles

Various mechanisms have been proposed to explain the inconsistency of the hadronic decay rates:

⊙ a destructive interference, due to the Fermi statistics, between the spectator antiquark $\bar{d}$ in the D^+ wave function and the identical $\bar{d}$ from the non–leptonic decay $c \to su\bar{d}$ [see Fig. 10(a)]. Since this interference does not occur neither for D^0 nor for D_s, the net result will be a reduction of $\Gamma(D^+)$. However a detailed calculation [58] shows that this mechanism, although contributing in the right direction, can only play a marginal role;

⊙ the contribution of the color–suppressed spectator diagrams. As one can realize comparing Fig. 9(a) and Fig. 10(a), for the D^0 and D_s decay the normal and the internal spectator diagrams are incoherent since they lead to different final states, then no interference is possible. On the contrary, both these D^+ decay diagrams lead to the same final states and then they can interfere. QCD shows that this interference is destructive, thus giving $\tau(D^\pm) > \tau(D^0) \approx \tau(D_s)$. Note that to accept this qualitative explanation one has to believe that the contribution from the internal spectator diagram is not really much suppressed by the color rule relative to the normal spectator amplitude. In spite of this funny thing, this mechanism of possible destructive interference between normal and internal spectator diagrams receive further support considering some Cabibbo–forbidden $D^\pm$ decays [59]. As already anticipated in the previous subsection, Cabibbo–suppressed decays occur when W $\to u\bar{s}$ (rather than W $\to u\bar{d}$) or c $\to d$

(rather than c $\rightarrow$ s). A careful examination of Fig. 9(a) and Fig. 10(a) shows that, in a D^+ decay, the c $\rightarrow$ d transition leads for both normal and internal spectator diagrams to the same final state quark configuration ($u\bar{d}d\bar{d}$) and then the two diagrams can interfere. On the contrary the W $\rightarrow$ $u\bar{s}$ transition leads for the normal spectator diagram to the $u\bar{s}s\bar{d}$ final state and to $s\bar{s}u\bar{d}$ for the internal spectator diagram. Then no interference is possible and hence:

$$\Gamma(c \rightarrow d) < \Gamma(W \rightarrow u\bar{s}) \tag{18}$$

The student is invited to check carefully the previous argument. With a proper quark pairing $\pi^+\pi^0$ and $\pi^+\rho^0$ are specific two-body final states arising from c $\rightarrow$ d while $K^+\bar{K}^0$, $K^+\bar{K}^{*0}$ and $\phi\pi^+$ are from W $\rightarrow$ $u\bar{s}$. Using the MARK II and MARK III measurements one gets $\Gamma(\pi^+\pi^0)/\Gamma(K^+\bar{K}^0)$ < 0.73 (90 % C.L.) which is not a very stringent test. However the hypothesis of destructive interference has an excellent confirmation by the E691 measurement [60] $\Gamma(\rho^0\pi^+)/\Gamma(\phi\pi^+) = 0.10\pm0.06$;

⊙ if the two non–spectator diagrams shown in Fig. 10(b) are not killed by helicity suppression, then $\Gamma(D^+)$ will be reduced relative to both $\Gamma(D^0)$ and $\Gamma(D_s)$ since the D^+ W–exchange diagram is the only Cabibbo–suppressed diagram. I have already mentioned a gluon emission from initial quarks as a possible mechanism invoked to overcome the helicity suppression. Another argument is put forward by Gibilisco and Preparata (GP [61]) who assume that non–leptonic decay of heavy flavors is dominated by long–distance effects. In this framework helicity suppression is avoided and W–exchange has a considerable weight for D^0 and D_s decay, its amplitude being comparable with the spectator amplitude. This would then be the reason of the difference in lifetime between the D^+ and D^0, D_s mesons.

Among the various models to descrive hadronic decays I have just mentioned the GP model: in the framework of the long–distance approach and using the meson wave–function of the Anisotropic ChromoDynamics (ACD) they obtain a satisfactory determination (in good agreement with the experimental data) of some exclusive non–leptonic decay widths of D, D_s and B mesons. In their approach the D^+ decay is completely parameter–free and thus they can compute successfully the widths of many decays. While disconnected (spectator) diagrams are calculated using form factors, the connected ones (W–exchange and annihilation) are parametrized in a suitable way; the parameters are obtained fitting some experimental widths and they are later used to predict some other channels. The overall agreement is satisfactory. A nice result is obtained for the decay $D_s \rightarrow \phi\pi^+$ for which there is no W–exchange contribution, thus allowing a completely parameter–free amplitude calculation. For this channel GP predict $\Gamma = 0.66$

10^{-11} s^{-1}, corresponding to a branching ratio of 2.9%, to be compared to a world average [53] of (2.8±0.5)%.

Another attempt to describe two–body non–leptonic decay of D mesons has been provided by Buccella et al. (BLMP [62]). They evaluate the amplitudes for two–body D meson non–leptonic decays using factorization and including short distance QCD corrections to next–to–leading order. Annihilation and W–exchange contributions are included as well as final state interactions; using SU(3) symmetry, the number of unknown parameters is greatly reduced. Fitting 25 experimental branching ratios with 6 parameters BLMP find an overall good agreement, but sizeable annihilation and W–exchange contributions (of the same order of magnitude for D^0 and D_s) are crucial to obtain agreement with experimental data.

Table 4: Comparison of BSW predicted branching ratios (in %) with experimental data.

Decay	BSW	BSW + annihilation	Experiment	PDG [53]
$D^0 \to K^- \rho^+$	12.5	13.8	13.0±1.3	7.3±1.1
$D^+ \to \bar{K}^0 \rho^+$	15.3		11.2±2.6	6.6±1.7
$D^0 \to \bar{K}^{*-} \pi^+$	3.7	9.1	7.4±1.3	4.5±0.6
$D^0 \to K^- \pi^+$	5.8		5.6±0.4	3.65±0.21
$D_s^+ \to \bar{K}^{*0} K^+$	1.6	2.4	4.8±2.4	2.6±0.5
$D^0 \to \bar{K}^0 \omega$	0.4	1.7	4.2±1.7	2.5±0.5
$D^+ \to \bar{K}^0 \pi^+$	3.6		4.1±0.6	2.6±0.4
$D_s^+ \to \phi \pi^+$	2.8	2.8	3.3±1.4	2.8±0.5
$D^+ \to \bar{K}^{*0} \pi^+$	0.3		2.7±1.8	1.9±0.7
$D^0 \to \bar{K}^0 \pi^0$	2.5		2.4±0.5	2.1±0.5
$D^0 \to \bar{K}^{*0} \pi^0$	1.4	3.9	2.0±0.9	2.1±1.0
$D^0 \to K^0 \eta$	0.4		2.0±0.9	< 2.3 (90% C.L.)
$D^0 \to K^0 \rho^0$	0.9	1.1	1.4±0.5	$(6.1\pm3.0)10^{-3}$
$D^0 \to K^0 \phi$	0.	1.0	$1.1^{+0.7}_{-0.5}$	$(8.8\pm1.2)10^{-3}$
$D^0 \to \bar{K}^{*0} \rho^0$	2.5		1.6±1.6	1.5±0.6

A milestone work in this domain is the model by Bauer, Stech and Wirbel

(BSW [63]). In this model the flavor flow in the non leptonic decay of a charm meson ($c\bar{q}$) is described by an effective interaction lagrangian of the form:

$$\mathcal{L}_{eff} = \frac{G}{\sqrt{2}}[a_1(\bar{u}d')_H(\bar{s}'c)_H + a_2(\bar{s}'d')_H(\bar{u}c)_H] \tag{19}$$

In other words, the short distance QCD interacting fields are replaced by their asymptotic fields. In this approach the scale dependent QCD coefficients C_1 and C_2 are replaced by new scale independent parameters a_1 and a_2 connected to C_1 and C_2 by the expressions:

$$a_1 \approx C_1 + \xi C_2 \qquad a_2 \approx C_2 + \xi C_1 \tag{20}$$

where ξ is a color factor arising from the color mismatch in forming color singlets. There are three classes of two–body decays: decays determined by a_1 only (normal spectator diagram), decays determined by a_2 only (internal spectator diagram) and decays where a_1 and a_2 amplitudes interfere. BSW extract the free parameters a_1 and a_2 from the $D \to K\pi$ branching fractions and find: a_1 = 1.3±0.1 and a_2 = -0.55±0.1. The negative sign of the ratio a_2/a_1 leads to negative interference in important exclusive D^+ decays. Since $a_1 \approx C_1(m_c)$ and $a_2 \approx C_2(m_c)$, this implies also $\xi \approx 0$, namely that quarks associated with different color singlet currents do not easily combine to form a single meson, while a naive expectation would suggest $\xi \approx 1/3$.

The results for a_1 and a_2 are used to calculate practically all two–body Cabibbo–favored and Cabibbo–suppressed D and D_s decay modes. Final state interactions and annihilation effects are taken into account. Some of the Cabibbo–favored results from BSW are reported in Table 4 in the same order as they appear in fig. 5(a) of [63]. The experimental branching ratios given in the table are the MARKIII and ARGUS results quoted in [63]. The agreement between the model and the experimental data is rather satisfactory. It is found that a sizeable part of the lifetime difference between D^0 and D^+ arises from the two–body decays due to the destructive interference in some important D^+ decay modes.

However the experimental data for D decays obtained from MARK III have been carefully reanalyzed by the Collaboration and the today results are quite different from those used by BSW. In particular the large fraction of two–body decays is not so large anymore. To give an idea of this change, I report in the last column of Table 4 the branching ratios obtained by the Particle Data Group [53]: it can be seen that in some cases they have moved a lot down.

Furthermore CLEO [64] has recently measured several D_s branching ratios that in the BSW model are predicted by a numerical factor multiplied by the parameter a_1. Then the model can predict ratios of branching ratios absolutely. Some of the new CLEO results are reported in Table 5, together with the corresponding BSW predictions. It should be noted that, in general, nearly all the other D_s decay modes are experimentally measured relative to the $\phi\pi$ decay

Table 5: D_s relative branching ratios compared to the BSW predictions. All the BR's are given relative to the decay mode $D_s \to \phi\pi^+$.

Decay	BSW	Experiment [64]
$(D_s \to \eta\pi^+)/(D_s \to \phi\pi^+)$	1.04	$0.54\pm0.09\pm0.06$
$(D_s \to \eta'\pi^+)/(D_s \to \phi\pi^+)$	0.61	$1.20\pm0.15\pm0.11$
$(D_s \to \eta\rho^+)/(D_s \to \phi\pi^+)$	1.96	$2.86\pm0.38\ ^{+0.36}_{-0.38}$
$(D_s \to \eta'\rho^+)/(D_s \to \phi\pi^+)$	0.56	$3.44\pm0.62\ ^{+0.44}_{-0.46}$
$(D_s \to \phi\rho^+)/(D_s \to \phi\pi^+)$	6.30	$1.86\pm0.26\ ^{+0.29}_{-0.40}$

mode, which is an uncertain anchor as none of its determinations are direct measurements. From Table 5 it is apparent that the BSW model practically fails to predict correctly all the modes.

4 CONCLUSIONS

I would like to close this brief experimental survey of heavy flavor characteristics grouping our present knowledge on their properties into three classes:

- ♠ successful: D–meson production mechanisms, lifetimes and branching fractions; some hints on few charm baryons; beauty characteristics (even if still in its infancy) and lifetimes;
- ♠ obscure: theory (or model) for hadronic c and b–flavored decays;
- ♠ occult: the large majority of charm and beauty baryons.

Many new techniques are being developed which may prove crucial to the study of heavy quark states. These include trigger processors, active targets, high resolution vertex detectors and improved devices for particle identification. It may well be that further innovation will be required for definite experiments.

However it seems to me that most of the future work is already on its way.

5 ACKNOWLEDGEMENTS

I am indebted for many stimulating and illuminating discussions on various topics related to this talk with M. Dameri, P. Morettini, F. Parodi, G. Ridolfi, I. Roncagliolo and L. Rossi.

I wish also to thank the Organizing Committee for the warm hospitality and for the perfect organization of this winter course. In particular I would like to express my gratitude to Prof. T. Bressani and Prof. G. Preparata for giving me the opportunity of a very enjoyable and fruitful meeting in this beautiful place.

References

[1] G. Altarelli and G. Parisi, *Nucl. Phys.* **B126** (1977) 298.

[2] G. Altarelli, CERN–TH 6623 (1992)

[3] M. Gluck, J. F. Owens and E. Reya, *Phys. Rev.* **D17** (1978) 2324.

[4] B. L. Combridge, *Nucl. Phys.* **B151** (1979) 429.

[5] J. Babcock, D. Sivers and S. Wolfram, *Phys. Rev.* **D18** (1978) 162.

[6] R. K. Ellis, Proceedings of the XXI Rencontre de Moriond: Strong Interactions and Gauge Theories, Les Arcs, France (1986).

[7] P. Nason, S. Dawson and R. K. Ellis, *Nucl. Phys.* **B303** (1988) 607.

[8] P. Nason, S. Dawson and R. K. Ellis, *Nucl. Phys.* **B327** (1989) 49.

[9] M. Mangano, P. Nason and G. Ridolfi, *Nucl. Phys.* **B373** (1992) 295.

[10] M. Mangano, P. Nason and G. Ridolfi, IFUP–TH–37/92, submitted to Nucl. Phys. B.

[11] P. N. Harriman, A. D. Martin, R. G. Roberts and W. J. Stirling, *Phys. Rev.* **D42** (1990) 798.

[12] P. J. Sutton, A. D. Martin, R. G. Roberts and W. J. Stirling, *Phys. Rev.* **D45** (1992) 2349.

[13] M. Aguilar–Benitez et al., *Nucl. Instr. and Meth.* **A258** (1987) 26.

[14] R. Ammar et al., *Phys. Lett.* **B183** (1986) 110.

[15] S. Aoki et al., *Phys. Lett.* **B187** (1987) 185.

[16] K. Kodama et al., *Phys. Lett.* **B263** (1991) 573.

[17] K. Kodama et al., *Phys. Lett.* **B284** (1992) 461.

[18] R. Bailey et al., *Z. Phys.* **C30** (1986) 51.

[19] R. Bailey et al., *Z. Phys.* **C28** (1985) 357.

[20] R. Bailey et al., *Nucl. Instr. and Meth.* **A213** (1983) 201.

[21] M. Adamovich et al., *Nucl. Instr. and Meth.* **A309** (1991) 401.

[22] J. R. Raab et al., *Phys. Rev.* **D37** (1988) 2391.

[23] D. J. Summers et al., Charm Physics at Fermilab, UMS/HEP/92–082. Please note that the quoted number of reconstructed charms is anticipated only.

[24] J. A. Apple, *Annu. Rev. Nucl. Part. Sci.* **42** (1992) 367.

[25] J. F. Gunion, *Phys. Lett.* **B88** (1979) 150.

[26] M. Aguilar–Benitez et al., *Nucl. Phys.* **B161** (1985) 400.

[27] S. Barlag et al., *Z. Phys.* **C39** (1988) 451.

[28] S. Barlag et al., *Z. Phys.* **C49** (1991) 555.

[29] Z. Wu, Ph.D. Thesis, Yale University, 1991 (unpublished).

[30] L. Rossi, INFN/AE–91/16, presented at the 4th International Symposium on Heavy Flavor Physics, Orsay (F), 25–29 June 1991.

[31] M. Adamovich et al., CERN–PRE 91–095.

[32] M. Aguilar–Benitez et al., *Z. Phys.* **C40** (1988) 321.

[33] M. Adamovich et al., CERN–EP 89–123.

[34] R. Ammar et al., *Phys. Rev. Lett.* **61** (1988) 2185.

[35] J. L. Ritchie et al., *Phys. Lett.* **B138** (1984) 213.

[36] D. S. Barton et al., *Phys. Rev.* **D27** (1983) 2580.

[37] L. Kluberg et al., *Phys. Rev.* **D38** (1977) 670.

[38] D. M. Alde et al., E772 Collaboration, *Phys. Rev. Lett.* **66** (1991) 133.

[39] M. E. Duffy et al., *Phys. Rev. Lett.* **55** (1985) 1816.

[40] H. Cobbaert et al., *Phys. Lett.* **B191** (1987) 456.

[41] C. Caso, Proceeding of the 1985 International Symposium on Lepton and Photon Interactions at High Energies, Kyoto (Japan), August 19–24, 1985, p. 488.

[42] M. Mac Dermott and S. Reucroft, *Phys. Lett.* **B184** (1987) 108.

[43] M. Adamovich et al., *Phys. Lett.* **B284** (1992) 453.

[44] J. N. Butler at al., Talk given at the XXVI International Conference on High Energy Physics, Dallas, Texas (USA), August 10–15, 1992.

[45] C. Albajar et al., *Phys. Lett.* **B256** (1991) 121, and *Phys. Lett.* **B256** (1991) 112.

[46] F. Abe et al., *Phys. Rev.* **D43** (1991) 664.

[47] J. Kroll, EFI 92–32, Talk presented at the XXVII Rencontres de Moriond, March 15–22, 1992

[48] J. P. Albanese et al., *Phys. Lett.* **B158** (1985) 186.

[49] K. Kodama et al., *Phys. Lett.* **B303** (1993) 359.

[50] N. R. Stanton, Talk given at the XXVI International Conference on High Energy Physics, Dallas, Texas (USA), August 10–15, 1992

[51] R. Fulton et al., *Phys. Rev.* **D43** (1991) 651.

[52] H. Albrecht et al., *Phys. Lett.* **B275** (1992) 195.

[53] K. Hisaka et al., Review of Particle Properties, *Phys. Rev.* **D45** (1992) 1.

[54] A. J. Weir et al., *Phys. Rev.* **D41** (1990) 1384.

[55] A. J. Buras, J. M. Gerard and R. Rückl, *Nucl. Phys.* **B268** (1986) 1626.

[56] J. F. Donoghue, *Phys. Rev.* **D33** (1986) 1516.

[57] J. Adler et al., *Phys. Rev. Lett.* **60** (1988) 1375.

[58] G. Altarelli and M. Maiani, *Phys. Lett.* **B118** (1982) 414.

[59] S. Stone, Charmed Meson Decays, HEPSY 1–92, to appear in "Heavy Flavors", edited by A. J. Buras and H. Lindner, World Scientific, Singapore (1992).

[60] J. C. Anjos et al., *Phys. Rev. Lett.* **62** (1989) 125.

[61] M. Gibilisco and G. Preparata, *Phys. Lett.* **B264** (1991) 207, MITH 92/9 (Submitted to Phys. Rev. D).

[62] F. Buccella, M. Lusignoli, G. Miele and A. Pugliese, *Z. Phys.* **C55** (1992) 243.

[63] M. Bauer, B. Stech and M. Wirbel, *Z. Phys.* **C34** (1987) 103.

[64] J. Alexander et al., *Phys. Rev. Lett.* **68** (1992) 1275, *Phys. Rev. Lett.* **68** (1992) 1279.